

# Fluorination of double-walled carbon nanotubes

H. Muramatsu,<sup>a</sup> Y. A. Kim,<sup>\*a</sup> T. Hayashi,<sup>a</sup> M. Endo,<sup>a</sup> A. Yonemoto,<sup>b</sup> H. Arikai,<sup>b</sup> F. Okino<sup>b</sup> and H. Touhara<sup>\*b</sup>

Received (in Cambridge, UK) 28th October 2004, Accepted 10th December 2004

First published as an Advance Article on the web 21st February 2005

DOI: 10.1039/b416393a

Fluorine atoms are selectively attached to the sidewall of the outer shell of DWNTs without disrupting the double-layered morphology; the stoichiometry of the fluorinated DWNTs is  $\text{CF}_{0.30}$ .

Double-walled carbon nanotubes (DWNTs),<sup>1</sup> which consist of two concentric cylindrical shells, have attracted the attention of numerous scientists because it is believed that these tubes are more thermally and chemically stable, and mechanically stronger when compared to single-walled carbon nanotubes (SWNTs). In addition, as with SWNTs, these double-layered tubes should behave as quantum wires due to their narrow diameters (*e.g.* <2 nm). One technical factor for limiting applications of carbon nanotubes is considered to be the difficulty of the preparation of high-dispersability nanotubes as in typical SWNTs. In this sense, extensive studies on chemical functionalization of carbon nanotubes have been carried out in recent years. Among various techniques, fluorination has been considered as a powerful tool of chemical functionalization for SWNTs,<sup>2</sup> resulting in high dispersability,<sup>3</sup> controlled electronic properties<sup>4</sup> and tube length.<sup>5</sup> In this account, DWNTs are fluorinated directly using elemental fluorine at 200 °C and the fluorinated tubes are characterized by X-ray photoelectron spectroscopy (XPS), high-resolution transmission electron microscopy (HR-TEM) and Raman spectroscopy. One of structural merits of DWNTs over SWNTs is that fluorine atoms can be attached to the outer shell of DWNTs selectively, leaving the inner shell of DWNTs intact, when the DWNTs used in this study have closed-end morphology.

Highly purified DWNTs in bundles were obtained by a catalytic chemical vapour deposition (CCVD) method and subsequent purification method. The synthesis of carbon nanotubes was carried out using a horizontal reactor. The Fe/MgO powder was placed at the center of the reactor, whereas Mo/Al<sub>2</sub>O<sub>3</sub> was placed at the furnace entrance. The reactor was heated to 875 °C in an Ar atmosphere. Subsequently, the carbon feedstock (CH<sub>4</sub> + Ar mixture, 1:1) was fed into the reactor (200 cm<sup>3</sup> min<sup>-1</sup>) for 10 min. A two-step purification process was applied to the synthesized products. An HCl treatment was used to remove the supporting catalyst material (MgO), followed by air oxidation at 500 °C for 30 min in order to remove amorphous carbon and chemically active SWNTs. Detailed experimental conditions have been described elsewhere.<sup>6</sup> Careful HRTEM observations confirmed a high yield of DWNTs (95%) in bundles. Fluorination of the highly purified DWNTs was carried out as follows. As a pretreatment, the tubes were heated at 200 °C under vacuum for several hours

in order to remove the residual oxygen gases and moisture. The DWNTs were fluorinated by the introduction of fluorine gas (1 atm) into the reaction chamber at 200 °C for 5 h. XPS Measurement (an Ulvac-phi model 5600) using non-monochromatized Mg-K $\alpha$  at 1253.6 eV, Raman study (a Kaiser HoloLab 5000 system) using a 532 nm Ar-ion laser line and HR-TEM observation (a JEOL JEM-2010FEF instrument) at 200 kV were carried out in order to characterize the fluorinated DWNTs.

Fig. 1 shows the C 1s spectra of the pristine and fluorinated DWNTs. An intense C 1s peak at 284.9 eV is assigned to sp<sup>2</sup> carbon whereas a weak C 1s peak at 288.9 eV is assigned to sp<sup>3</sup> carbon which is covalently bound to fluorine atoms. As shown in Fig. 1(b), the only F 1s peak observed is assigned to covalent C–F bonds (687.75 eV). The stoichiometry of the fluorinated DWNTs (CF<sub>0.30</sub>) was determined by dividing the integrated intensity of the C 1s peak by the integrated intensity of the F 1s peak.<sup>7</sup> An agreement between the ratio of the integrated intensities of the two C 1s peaks (C 1s<sub>288.9</sub>/C 1s<sub>all</sub> = 0.32) and the ratio of the integrated intensities of the C 1s and F 1s peaks (F/C ratio = 0.30) is an indirect indication for fluorine attachment to the outer shell of DWNTs, leaving the inner shell intact, because it is expected that our DWNTs have a closed-tip morphology. It is known that fluorinated SWNTs show a low conductivity and the binding energies have to be calibrated due to charging effects during XPS measurement. The absence of a charging effect for our fluorinated DWNTs suggests that no significant degradation of the sample occurs possibly due to sustainment of the inner shells of the DWNTs.

According to a low-resolution TEM study (Fig. 2 (a)) our DWNTs exist mainly in a bundle state, and the diameters of the DWNT bundles are in the range of 10–50 nm. In addition, typical

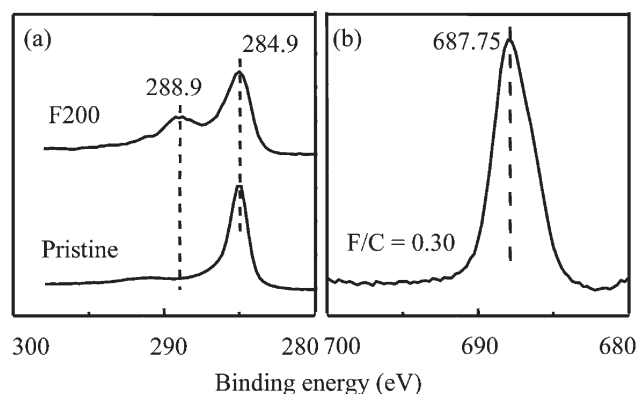
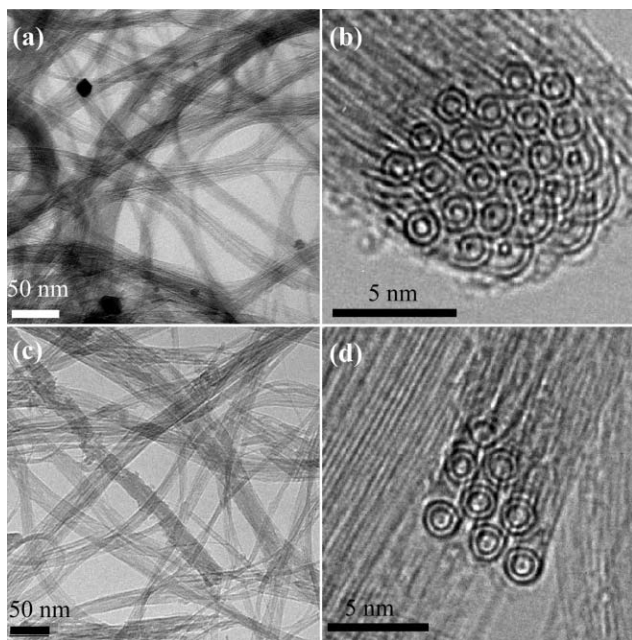


Fig. 1 C 1s XPS (a) and F 1s XPS (b) spectra of pristine and fluorinated (F200) DWNTs.

\*yak@endomoribu.shinshu-u.ac.jp (Y. A. Kim)  
htohara@giptc.shinshu-u.ac.jp (H. Touhara)



**Fig. 2** Low-resolution (a) and high-resolution cross-sectional (b) TEM images of the pristine DWNTs and low-resolution (c) and high-resolution cross-sectional (d) TEM images of the fluorinated DWNTs.

cross-sectional HR-TEM images of DWNTs show that they are hexagonally packed in bundles (Fig. 2(b)). No distinctive change in macro-morphology of DWNTs is found through fluorination (Fig. 2(c)). It is noteworthy that double-layered cylindrical shells are clearly seen (Fig. 2(d)) according to high-resolution cross-sectional images of the fluorinated DWNTs. Furthermore, the hexagonal packing structure is disturbed, possibly due to chemically incorporated fluorine atoms on the outer shells of DWNTs.

Raman spectroscopy has been extensively used to characterize carbon nanotubes because this technique is very sensitive to structural disorder and diameters of nanotubes.<sup>8</sup> Low-frequency Raman spectra on the pristine and fluorinated DWNTs (Fig. 3(a)) were measured in order to determine the radial breathing mode (RBM) frequency, which is inversely related to tube diameter. Raman lines appear above  $250\text{ cm}^{-1}$  (corresponding to the inner shell of DWNTs), and below  $250\text{ cm}^{-1}$  (associated with the outer

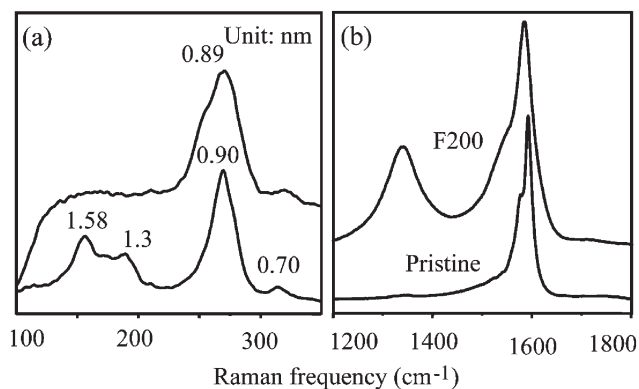


**Fig. 3** Low-frequency (a) and high-frequency (b) Raman scattering of the pristine and the fluorinated (F200) DWNTs.

shell of DWNTs). The tube diameters (see numerical values inserted in Fig. 3(a)) are calculated from the RBM frequencies using the equation  $\omega_{\text{RBM}} = 234/d_t + 10$ ,<sup>9</sup> where  $d_t$  is the tube diameter (nm) and  $\omega_{\text{RBM}}$ , the RBM frequency ( $\text{cm}^{-1}$ ). It is confirmed that the pristine sample consists of two pairs of DWNTs; (inner tube:outer tube = 0.7:1.3 and 0.9:1.58, respectively). Even though there was no significant change for peaks at *ca.* 270 and  $324\text{ cm}^{-1}$  corresponding to inner shells, the RBM frequencies originating from the outer shells of DWNTs is clearly depressed through fluorination. We note also that a double-layered morphology of the fluorinated DWNTs is clearly seen by the cross-sectional HR-TEM observation. The depression of the RBM frequencies, corresponding to large-sized diameters (1.58 and 1.3 nm), re-confirmed that the tubes used in this study consist of *two* concentric shells with the outer shell acting as a protective layer from chemical attack of fluorine gas, leaving the inner shell intact (it is supposed that our DWNTs have end-closed morphology). If each RBM is derived from SWNTs, RBM corresponding to smaller sized tubes should disappear due to higher reactivity. Therefore, Raman study on fluorinated nanotubes is a useful way to discriminate DWNTs over other types of nanotubes because a CCVD synthesis can produce mixtures of DWNTs and SWNTs either in an isolated or in a bundle state. For our samples, it is confirmed that the DWNTs used in this study exhibit high purity with a minimal portion of SWNTs. Fig. 3(b) shows high-frequency Raman spectra of the pristine and fluorinated DWNTs. Through fluorination, a slightly decreased Raman frequency of the G band at  $1590\text{ cm}^{-1}$  (associated with the  $E_{2g2}$  mode), a highly intensified D band at  $1346\text{ cm}^{-1}$  (the defect mode) and highly increased *R* value (the intensity of D band divided by the intensity of G band) indicate that chemical attachment of fluorine to the DWNTs induces structural distortion of the outer concentric shells due to incorporation of  $\text{sp}^3$  hybridization as in fluorinated SWNTs.<sup>2</sup> The lower *R* value ( $R = 0.45$ ) of the fluorinated DWNTs than that of the fluorinated SWNTs ( $R = 0.85$ ) (which was obtained at same conditions using the same fluorination apparatus) also indicate indirectly that the inner shells of our DWNTs are intact after fluorination.

In summary, we successfully attached fluorine atoms to the sidewall of the outer shell in DWNTs through direct reaction with fluorine gas at  $200\text{ }^\circ\text{C}$  for 5 h. The stoichiometry of the fluorinated DWNTs is  $\text{CF}_{0.30}$ , based on XPS study, while double-layered structure is sustained after fluorination according to HR-TEM observation. The depression of RBM and high intensity of D bands, originated from the outer shells of DWNTs, are ascribed to geometrical changes from round to distorted cross-sectional shape due to incorporation of  $\text{sp}^3$  hybridization. From the above studies, it is clear that fluorination is a powerful tool to distinguish DWNTs from SWNTs. In addition, it is expected that tube morphology is sustained at higher fluorination temperature above  $200\text{ }^\circ\text{C}$  due to their higher structural stability than that of SWNTs. By tuning the electronic property of only the outer shell and controlling the dispersability of DWNTs without disrupting the double-layered concentric shell morphology through fluorination, we envisage these chemically modified DWNTs to be useful in the fabrication of novel sensors, nanocomposites and electronic devices.

This work was supported by the CLUSTER of Ministry of Education, Culture, Sports, Science and Technology.

H. Muramatsu,<sup>a</sup> Y. A. Kim,<sup>\*a</sup> T. Hayashi,<sup>a</sup> M. Endo,<sup>a</sup> A. Yonemoto,<sup>b</sup>  
H. Arikai,<sup>b</sup> F. Okino<sup>b</sup> and H. Touhara<sup>\*b</sup>

<sup>a</sup>Faculty of Engineering, Shinshu University, 4-17-1 Wakasato,

Nagano-shi, 380-8663, Japan. E-mail: yak@endomoribu.shinshu-u.ac.jp

<sup>b</sup>Faculty of Textile Science and Technology, Shinshu University, 3-15-1  
Tokida, Ueda 386-8567, Japan. E-mail: htouhara@giptc.shinshu-u.ac.jp

## Notes and references

- 1 A. Oberlin, M. Endo and T. Koyama, *J. Cryst. Growth*, 1976, **32**, 335; S. Bandow, M. Takizawa, K. Hirahara, M. Yudasaka and I. Iijima, *Chem. Phys. Lett.*, 2001, **337**, 48; E. Flahaut, R. Basca, A. Peigney and C. Laurent, *Chem. Commun.*, 2003, 1442; S. C. Lyu, T. J. Lee, C. W. Yang and C. J. Lee, *Chem. Commun.*, 2003, 1404; T. Sugai, H. Yoshida, T. Shimada, T. Okazaki and H. Shinohara, *Nano Lett.*, 2003, **3**, 769; M. Endo, T. Hayashi, H. Muramatsu, Y. A. Kim, H. Terrones, M. Terrones and M. S. Dresselhaus, *Nano Lett.*, 2004, **4**, 1451.
- 2 E. T. Mickelson, C. B. Huffman, A. G. Rinzler, R. E. Smalley, R. H. Hauge and J. L. Margrave, *Chem. Phys. Lett.*, 1998, **296**, 188; K. H. An, J. G. Heo, G. K. Jeon, D. J. Bae, C. Jo, C. W. Yang, C. Y. Park, Y. H. Lee, Y. S. Lee and Y. S. Chung, *Appl. Phys. Lett.*, 2002, **80**, 4235; S. Kawasaki, K. Komatsu, F. Okino, H. Tohara and H. Kataura, *Phys. Chem. Chem. Phys.*, 2004, **5**, 1769.
- 3 E. T. Mickelson, I. W. Chiang, J. L. Zimmerman, P. J. Boul, J. Lozano, J. Liu, R. E. Smalley, R. H. Hauge and J. L. Margrave, *J. Phys. Chem. B*, 1999, **103**, 4318.
- 4 K. N. Kudin, H. F. Bettinger and G. E. Scuseria, *Phys. Rev. B*, 2001, **63**, 45413.
- 5 Z. Gu, H. Peng, R. H. Hauge, R. E. Smalley and J. L. Margrave, *Nano Lett.*, 2002, **2**, 1009.
- 6 Y. A. Kim, H. Muramatsu, T. Hayashi, M. Endo, M. Terrones and M. S. Dresselhaus, *Chem. Phys. Lett.*, 2004, **398**, 87.
- 7 S. Kawasaki, T. Aketa, F. Okino, H. Touhara, O. V. Boltalina, I. V. Gol'dt, S. I. Troyanov and R. Taylor, *J. Phys. Chem. B*, 1999, **103**, 1223; N. Liu, H. Touhara, F. Okino and S. Kawasaki, *J. Electrochem. Soc.*, 1996, **143**, 2267.
- 8 A. M. Rao, E. Richter, S. Bandow, B. Chase, P. C. Eklund, K. A. Williams, S. Fang, K. R. Subbaswamy, M. Menon, A. Thess, R. E. Smalley, G. Dresselhaus and M. S. Dresselhaus, *Science*, 1998, **275**, 187; M. S. Dresselhaus and G. Dresselhaus, *Adv. Phys.*, 2002, **51**, 1.
- 9 A. Jorio, R. Saito, J. H. Hafner, C. M. Lieber, M. Hunter, T. McClure, G. Dresselhaus and M. S. Dresselhaus, *Phys. Rev. B*, 2001, **86**, 1118.